Optimization of Waterjet Propulsion for High-Speed Ships

L. ARCAND* AND C. R. COMOLLI†
Pratt & Whitney Aircraft Division of United Aircraft Corporation, West Palm Beach, Fla.

Gas turbine-waterjet propulsion offers significant advantages in many high-speed or special purpose ships, which generally have speed capability above 30 knots and installed power-to-weight ratios above 10 hp per full-load ton. Included are destroyers of the destroyer (DD) type and some smaller destroyer leaders (DL), hydrofoils above 40 knots, surface effect ships, and planing craft. Optimization of gas turbine-waterjet installations for maximum net thrust (system thrust less drag associated with propulsion system) depends primarily on the *L/D* ratio of the basic hull, design speed, ship length, and component efficiencies. The major components are the inlet, pump, gearbox, gas turbine, and associated required auxiliaries. For high-speed ships, propulsive coefficients of 60–65% are possible with conservative component-loss assumptions.

Nomenclature

C_D	=	drag coefficient, $C_D = D/A_{\text{inlet}}(\rho V^2/2g)$
D	=	drag, lb
g	=	gravitational constant, ft/sec^2
h	=	inlet lip height, ft
H	=	head, ft/H_2O
H_{si}	=	head, static inlet, ft
H_{sx}	=	head, static hull, ft
H_{to}	=	head, total, freestream, ft
H_{t1}	=	head, total inlet, ft
H_{t2}	=	head, total, diffuser exit, ft
L	=	waterline length, ft
L/D	=	lift/drag ratio
N	=	shaft speed, rpm
NPSH	=	net positive suction head (total head above the vapor pressure at waterjet inlet), ft
N_s	=	specific speed, $N(\text{gal/min})^{1/2}/\Delta H^{3/4}$
PC	=	propulsive coefficient, $TV/\text{shp} \times 550$
Q	=	flow rate, gal/min
R	=	radius, in.
S	=	suction specific speed, $N(Q)^{1/2}/\text{NPSH}^{3/4}$
sfc	=	specific fuel consumption, lb/hp-hr
shp	=	shaft horsepower
T	=	thrust, lbf
v	=	local velocity, fps
V_{im}	=	mean inlet velocity, fps
V_J	=	jet velocity, fps
V_k	=	velocity of vehicle, knots
V_o	=	freestream velocity, fps
V_1	=	inlet velocity, fps
$\dot{w}$	=	flow rate, lb/sec
W	=	weight, lb
x	=	distance from bow to inlet, ft
y	=	distance perpendicular to hull or flow boundary layer, ft
δ	=	boundary-layer thickness, ft
Δ	=	displacement, long tons (2240 lb)
η_p	=	pump efficiency, %
θ	=	momentum thickness
ΔH	=	pump total head rise, ft
θGB	=	gearbox efficiency, $\text{shp}_{\text{out}}/\text{shp}_{\text{in}}$, %

Introduction

SEAGOING propulsion with gas-turbine powered waterjets has received increasing acceptance in recent years. The modified aircraft gas turbine is chosen as a powerplant because of its light weight and high power density, both critical in high-speed ships, which have relatively low lift/drag ratios. As the speed of a vessel increases, weight becomes critical if useful payload is to result. There are various reasons for choosing a waterjet. In landing craft, absence of propeller damage and improved maneuverability are of major importance. In other vehicles improved work efficiency, compared to the propeller-driven vehicle, is the overriding reason. Frequently, the reason for the selection is to eliminate lengthy, expensive power trains. In the final analysis, the waterjet is selected when it will do the task at lower total cost, whether this results from improved reliability, better work efficiency, lower maintenance, or lower installed cost.

This paper identifies some applications where waterjets promise better over-all effectiveness than propeller systems. A typical gas turbine-waterjet propulsion system is shown in Fig. 1. The gas generator, which is an aircraft gas turbine modified for marine use, delivers hot gas to a free turbine. Turbine power is delivered to a large water pump, which accepts water from the inlet, raises its energy, and discharges it through a nozzle. Advantages are higher power per unit weight, lower vessel drag per unit thrust, increased payload fraction, and reduced horsepower required. Determining when advantages outweigh disadvantages is the subject of the propulsion optimization program.

System Optimization

Basic Approach

The approach used to select waterjets is an iterative solution of the net thrust equation for varying inputs. The powerplant is optimized when the ship thrust requirement is satisfied at minimum shaft horsepower. This is essentially the same technique as that of Refs. 1 and 2, except that in large displacement ships, boundary-layer ingestion effects alter

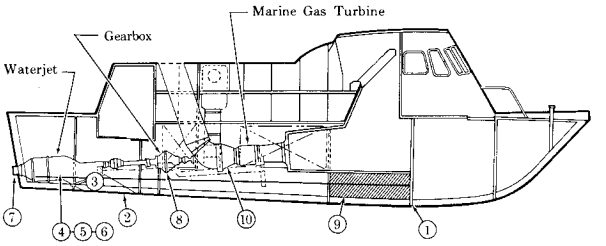

1 Bare Hull Drag
2 External Drag of Inlet
3 Inlet Energy Loss
4 Drag Due to Machinery Weight
5 Drag Due to Contained Water Weight
6 Pump Efficiency
7 Nozzle Loss Coefficient
8 Gearbox Efficiency
9 Drag Due to Fuel Weight
10 Engine Performance

Fig. 1 Powerplant optimization considerations.

Presented as Paper 67-350 at the AIAA/SNAME Advance Marine Vehicles Meeting, Norfolk, Va., May 22–24, 1967; submitted May 29, 1967; revision received November 16, 1967.

* Assistant Project Engineer, Florida Research and Development Center.

† Project Engineer, Florida Research and Development Center.

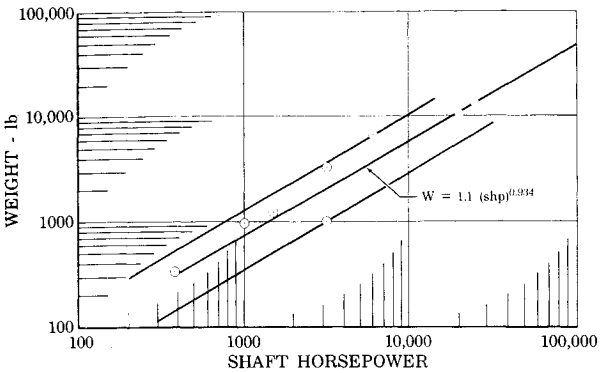

Fig. 2 Marine gas turbine weight (at maximum continuous power) vs shaft horsepower.

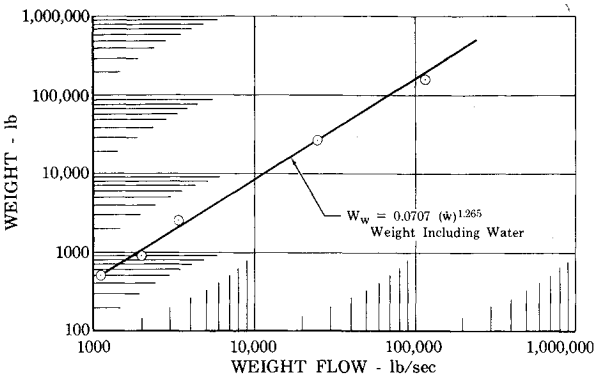

Fig. 4 Waterjet weight vs flow rate.

the solution appreciably. As will be shown, minimum shaft horsepower is not always a proper criterion for choosing propulsors, although its calculation yields a maximum practical propulsive coefficient based on machinery performance, weight estimates, and component performance.

Figure 1 shows the items to be optimized. Item 1 is the drag of the hull at design speed without conventional propulsion system appendages, rudders, bearings, struts, and propeller shafts. Item 2, the external drag of the waterjet inlet, is that drag in excess of the smooth (unpierced) hull drag. It consists of friction drag from any increased hull surface exposed to flow, interference drag generated at the "corners" the inlet makes with the hull, and any profile drag from external diffusion. It is the least definitive term in the optimization. Item 3 is the inlet energy loss coefficient that represents the dynamic head loss of the water in the induction system, plus a term to reflect elevation of the water. Elevation loss is generally negligible in displacement hulls but can be significant in hydrofoils. Item 4, the additive drag due to machinery weight, is the estimated weight of the prime mover, gearbox, waterjet and associated ducts, stacks, and fundations divided by the lift/drag ratio of the hull. Item 5 is the drag associated with weight of the water in the system divided by the lift/drag ratio of the hull. Although one may argue that water contained below the waterline of the hull has no weight effect, since it occupies space and communicates with the sea, it represents a lost buoyancy term and we account for it as a dead weight. Pump efficiency, item 6, is the over-all mechanical efficiency, $\eta_p = (\Delta H\dot{w})/550$ shp. Typical efficiency values for the region of interest to waterjet designers are 85 to 90% with the lower number for relatively lower-power machines. Nozzle loss coefficient, item 7, is the energy loss coefficient of the nozzle, typically about 2% of the velocity head. Gearbox efficiency, item 8; additive drag due to fuel weight, item 9; and prime mover sfc, item 10, are obvious influence factors.

As previously mentioned, in finding minimum installed horsepower we must calculate the maximum net thrust of the system—the thrust required to move the ship and payload less the thrust to move the propulsion machinery and fuel. For preliminary design purposes, estimates of weights of the various components are required. Figures 2–4 are weight curves used in this study for gas-turbine weight as a function of power, gearbox weight as a function of shp, and waterjet weights as a function of flow rate. These curves are from data on existing and proposed machinery. The gearbox weight curve, which is for marine and aircraft practice, assumes a simple nonreversing gearbox with a reduction ratio of 4:1. This implies relatively high waterjet rotational speeds. In our studies, particularly of low-speed ships at low shaft horsepower, we find that low rotational speed leads to waterjets that approach ducted propellers or pump jets. This has resulted in our arbitrary definition of waterjets as those that operate at a pump specific speed of $N_s \leq 10{,}000$, where as higher optimized values are considered either pump jets or propellers.

Typical Results

Typical study results for displacement hulls, using the pump speed limits and weight estimates, are plotted in Fig. 5 as propulsive coefficient vs displacement/drag ratio for various speeds with a fixed boundary-layer condition. Figure 6, containing more general curves, show typical values for different types of craft and propulsion systems. In arriving at these curves, waterjet weight is taken as twice the wet-weight value shown in Fig. 4, to account for the weight of water in inlet ducting to the pump. Also, the weight of the entire propulsion system is increased by 20% to account for machinery foundations, miscellaneous auxiliaries, and stacks chargeable to the propulsion system.

In the particular cases shown, the ship length is 400 ft and the inlet is positioned at 90% of the ship length. The latter is

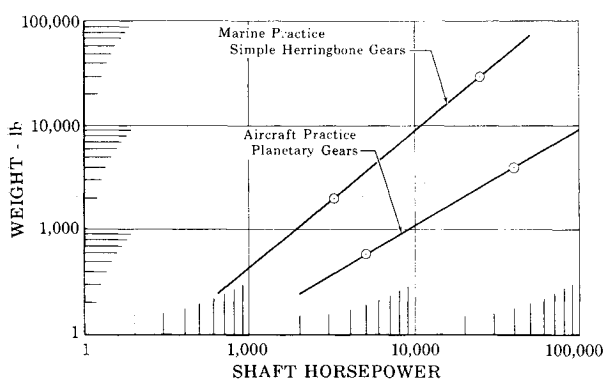

Fig. 3 Gearbox weights for waterjets (reduction ratio ≈ 4/1).

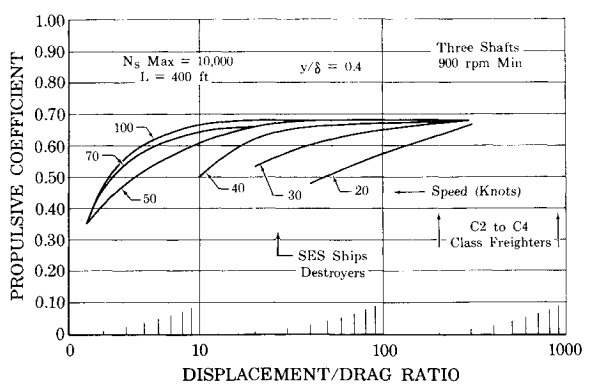

Fig. 5 Optimum gas turbine waterjet propulsive coefficients vs displacement/drag ratio.

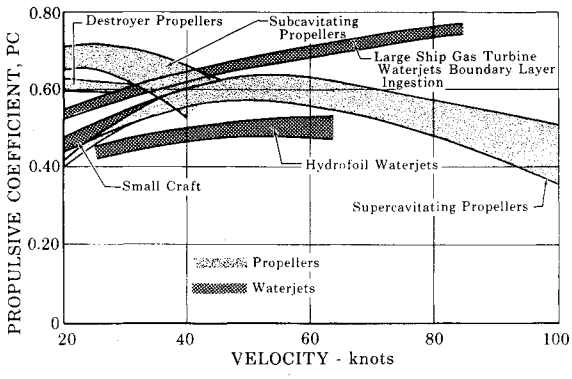

Fig. 6 Design propulsor comparisons.

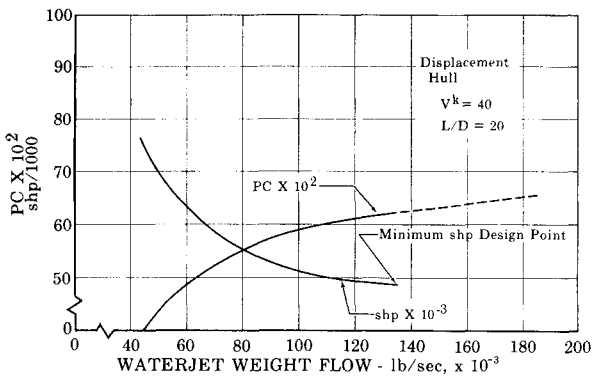

Fig. 8 Typical printout during optimization.

important in a displacement hull, because it determines the momentum of the boundary-layer flow available to the propulsor. In the case of hydrofoils or planing hulls, there is usually no available, coherent, boundary-layer flow, so ship length is not a consideration.

The boundary-layer velocity distribution used is Von Karman's description of turbulent flow, $v/V_o = (y/\delta)^{1/9}$. The definition of boundary-layer thickness used is an approximation of the Schoenherr-Von Karman development, $\delta/x = 0.02065 - 0.00138 \log_{10}(V_K \cdot x)$. It is quite accurate at $\log_{10}(V_K \cdot x)$ above 2.8 and open sea temperatures. δ/x typically ranges from 0.014 to 0.017.

The importance of the ingestion of the boundary layer is shown in Fig. 7. In this figure waterjets for an 80-knot, 350-ft ship were optimized for different ingestion percentages without considering geometric limits. It shows a possible variation in propulsive coefficients from approximately 81% at 10% ingestion to 70% at 40% ingestion. In most cases studied an inlet that ingested only 10% of the boundary layer resulted in unrealistic geometries with inlets wider than the ship. A realistic condition is $y/\delta = 0.4$.

The reason that propulsive coefficient is sensitive to boundary-layer suction has been discussed by Wislicenus,[3] Gearhart,[7] Thurston,[6] and others. Wislicenus points out that thrust is proportional to $V_J - V_I$ at a fixed flow rate through the propulsor whereas required power is proportional to $V_J^2 - V_I^2$. Therefore, at a fixed thrust and flow rate, the propulsor with the lower inlet velocity (relative to the propulsor) will require less shaft work.

For decades, naval architects have been faced with boundary-layer effects that skew the velocity profile of the water that is approaching the propeller. In the case of propeller-hull matching, the velocity profile is a problem because the blade faces varying angles of attack in each revolution, resulting in varying blade loading. In a waterjet installation, the flow is decelerated and turned parallel to the shaft, thus approaching the rotor with a more uniform velocity profile.

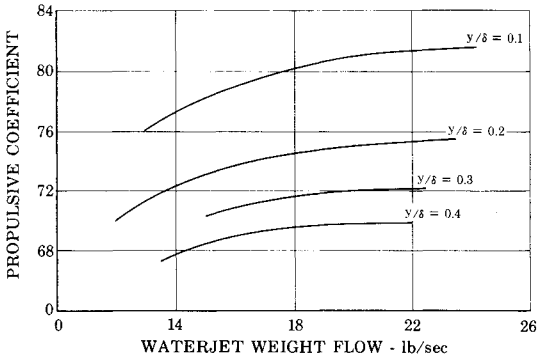

Fig. 7 Importance of the efficient ingestion of the boundary layer (80 knots, 350-ft ship).

Optimization was done on a small engineering computer by a simple iterative procedure in which flow is incremented and the power plant "redesigned" in each step until the minimum installed power is ascertained. The program optimizes a ship and speed at various lift/drag ratios for each case. It can include mission capabilities by specifying sfc and endurance for several power settings. In this way, optimization takes into account fuel weight, which generally reduces optimum propulsive coefficient by a small amount (on the order of 2%). The program loop uses some engineering approximations for input. For example, choice of $y/\delta = 0.1$ would almost always result in early abort of the calculation at a low propulsive coefficient and high shaft horsepower. Typical results are shown in Fig. 8.

Inlet Design

Three technical areas of interest in inlet diffuser design are 1) external drag, 2) internal performance, and 3) cavitation as it affects performance and structural damage.

External drag

External drag of a waterjet inlet is one of the most important inputs to the propulsor optimization program. Unfortunately, only limited information is available. Data for airplane inlets[4,5] generally are for relatively low Reynolds numbers with thin boundary layers. Marine data are limited to condenser inlets, with several exceptions, none of which provides information in the area of interest. The problem is to minimize the external drag while minimizing internal losses to avoid cavitation. In studying inlets, we consider only external drag as a drag term and classify "internal drag" as an energy loss chargeable to the waterjet. This differs from methods of condenser designers, who consider both as drag terms. The net effect is the same, i.e., to increase horsepower above the ideal (bare hull) value. External drag consists of viscous drag due to any added surface area, interference drag at the intersections of the hull and the inlet, and any ram drag from external diffusion forward of the inlet.

Two types of displacement hull inlets are submerged or flush (Fig. 9) and extended or scoop. Most current displacement hull waterjets utilize the flush inlet. According to Hoerner[5] such inlets provide zero external drag. In addition, they lend themselves to incorporation into the waterjet inlet casing and

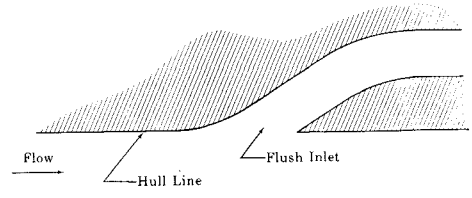

Fig. 9 Typical flush inlet design.

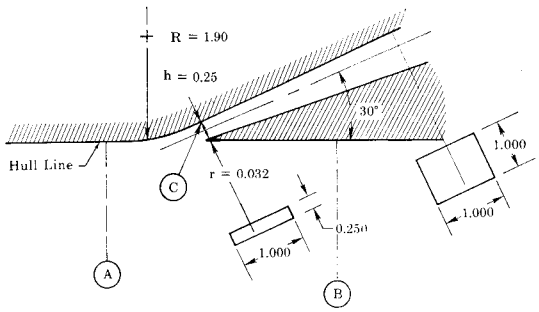

Fig. 10 Baseline flush inlet model; expansion ratio 4/1, inlet aspect ratio = 4.

permit easy installation in small craft. Disadvantages are relatively high internal loss coefficient, and susceptibility to cavitation, although our early experiments indicate that these inlets have the least drag of the candidates.

To study inlet external drag, we used a small wind tunnel to simulate the velocity ratio and boundary-layer profile for typical operating conditions. Our baseline test unit is two-dimensional with a flush inlet followed by a rectangular diffuser as sketched in Fig. 10. Figure 11 is a photo of the test setup. In addition we used a baseline scoop inlet, as shown in Fig. 12. Both units established measurement techniques and provided primary data on easily reproducible configurations.

Drag data for these inlets are shown in Figs. 13a and 13b. We call these results *apparent* external drag coefficient, because they compare the momentum downstream of the inlet to the momentum of the undisturbed flow at the same location. This is the technique used by Mossman and Randall.[4] The *real* external drag of the inlet takes into account the ideal downstream momentum (assuming perfect two-dimensional ingestion) and compares it to the actual or measured downstream momentum.

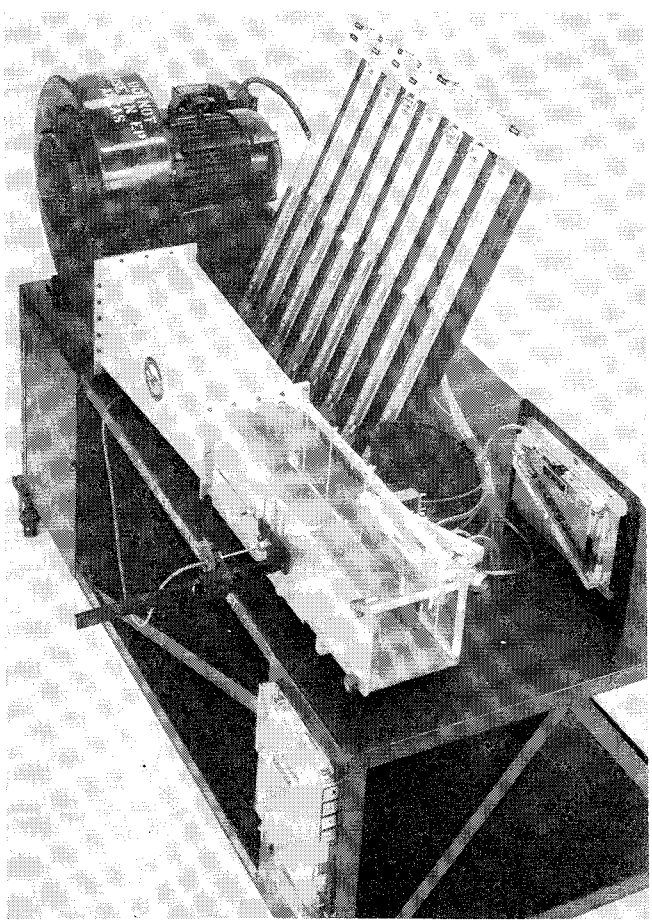

Fig. 11 Baseline test unit.

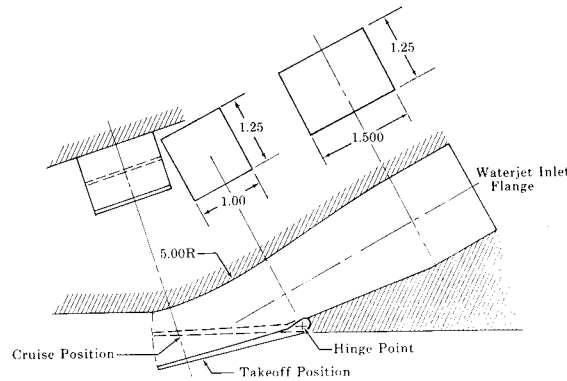

Fig. 12 Variable-area inlet model.

In studying the apparent drag of the two inlets, the following items were noted:

1) The flush inlet has lower drag than the scoop, almost exclusively because of the sharp corner interference drag of the scoop. (Future experiments will add cruise position fairings that fill in the sharp corners.)

2) The closer the inlet velocity is to the freestream velocity, the lower the drag. This indicates that flow is spilling over the inlet at most conditions.

3) The thicker the boundary layer is with respect to inlet lip height, the lower the drag, although the flush data do not demonstrate this consistently.

In studying the flow data for the flush inlet, we compared V_{im} to an ideal V_1 based on two-dimensional ingestion of a portion of the boundary layer upstream. Ideal ingestion would occur if all flow entered the inlet in the axial direction of motion. In the cases studied, V_1 (ideal) was higher than V_{im},

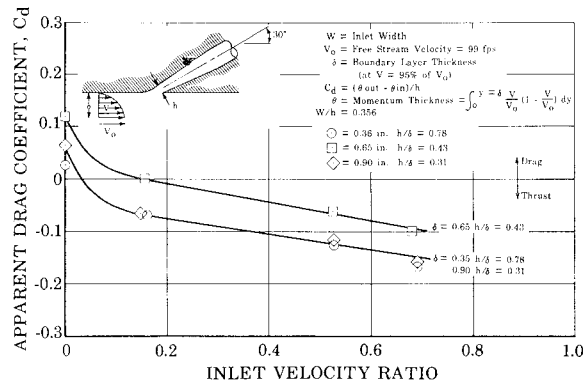

a) Flush inlet

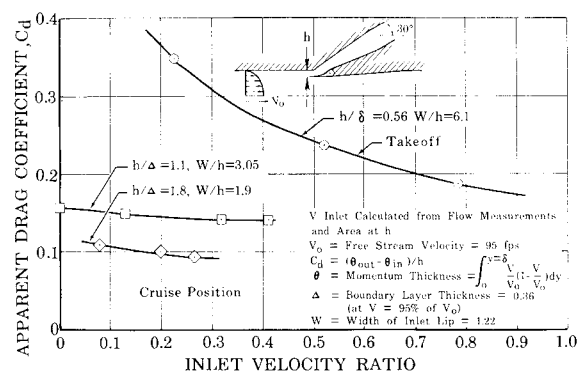

b) Scoop inlet

Fig. 13 Apparent drag coefficient vs velocity ratio for flush inlet.

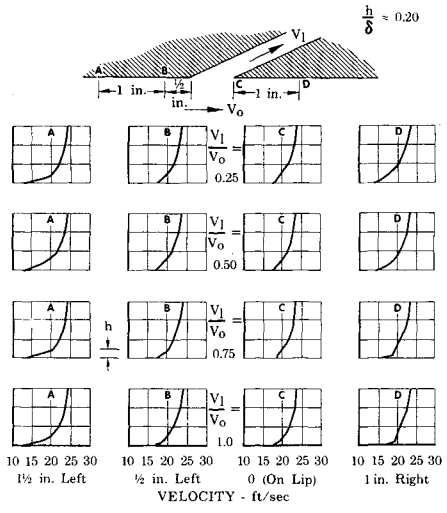

Fig. 14 Centerline velocity distributions—low-speed test.

which indicates that the flow is ingested from areas ahead of and on both sides of the inlet. In this respect, the flush inlet will have a better performance than the scoop inlet, since it will tend to ingest more of the low-velocity flow near the hull than the comparable scoop inlet. This results in lower drag, since the drag-affected area will "see" lower velocities than the comparable scoop.

To show how a negative drag coefficient can be obtained, information is given in Fig. 14 for line velocity profiles for four velocity ratios from an early test of a flush inlet. In most cases, the flow downstream (C and D) has a thinner boundary layer than the approach flow. The effect is more noticeable as the velocity ratio increases. In calculating a real drag coefficient, we believe the actual profile at D should be compared to an ideal profile at D. We integrate these profiles over the entire affected area downstream, which we

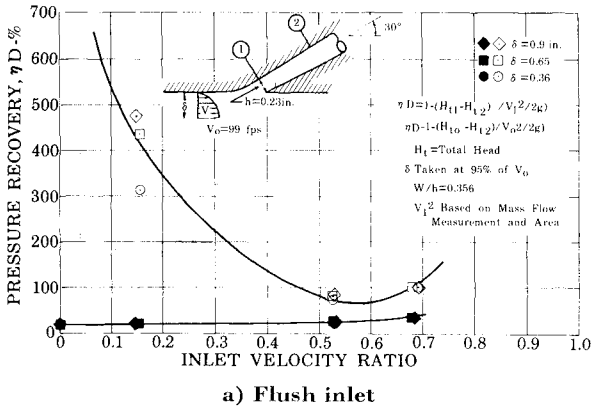

a) Flush inlet

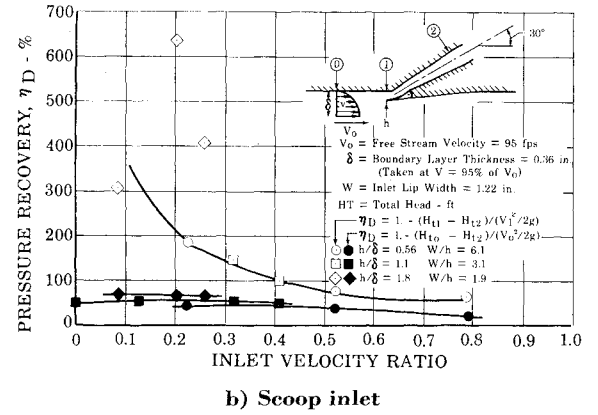

b) Scoop inlet

Fig. 15 Pressure recovery vs velocity ratio for flush inlet.

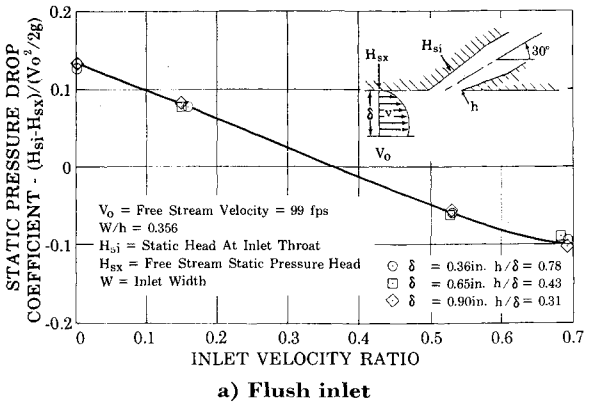

a) Flush inlet

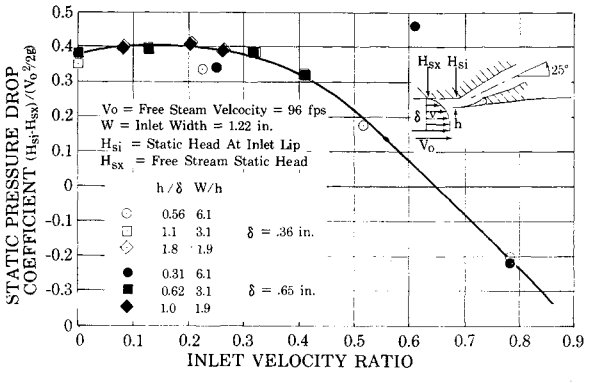

b) Scoop inlet

Fig. 16 Static pressure drop coefficient vs velocity ratio for flush inlet.

find is $1\frac{1}{2}$ inlet widths on either side of the centerline at a distance of 4 widths downstream of the inlet lip.

Internal performance

The internal performance of an inlet diffuser system is critical to the over-all system performance since each foot of head lost here must be made up by the pump. We define the efficiency of an inlet diffuser as

$$1 - (H_{t1} - H_{t2})/(V_1^2/2g)$$

where $V_1^2/2g$ = velocity head available for diffusion.

We plot this efficiency in two ways. One, based on the measured inlet velocity V_{im} with $V_{im}^2/2g$ as the available velocity head, and the other a freestream efficiency with V_o as the available velocity. Results are shown in Figs. 15a and 15b. The apparent pressure recovery or efficiency goes above 100% at low velocity ratios, indicating that V_{im} measured from inlet area and flow measurements is higher than calculated. This implies separation at the inlet, causing the in-

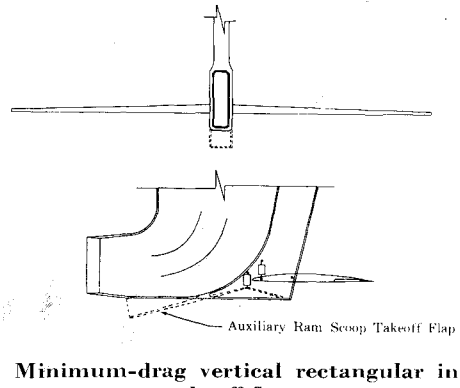

Fig. 17 Minimum-drag vertical rectangular inlet with takeoff flap.

gested flow to have higher local velocity than calculated. When we refer our performance to freestream conditions, diffuser efficiency becomes quite low, as might be expected in a thick boundary layer. Neither measurement is adequate, although the freestream efficiency lends itself better to design calculations than does the apparent efficiency.

The scoop inlet (as expected) is a better pressure recovery device than is the flush inlet. Also, the greater the scoop extension is, the better the pressure recovery. Examination of scoop data comparing cruise to takeoff position recovery also shows that efficient diffusion of a nonuniform velocity is inherently difficult, particularly at the smaller percentages of the boundary-layer flow. However, the efficiencies shown, together with associated drag characteristics, indicate trends only and are not acceptable values for a real installation because of the relatively crude models used. Thus the inclination angles used of 25° and 30° were arbitrarily chosen to make the inlet system as short as possible. The diffusers were made rectangular to avoid the transition problem between the rectangular lip and the circular diffuser.

Cavitation

Compromises made to avoid cavitation, both internal and external, may result in poor pressure recovery or high drag. This is particularly true at the high speeds (50–100 knots) contemplated for future ships. Internally, we would expect the lowest static pressure on the suction surface of the inlet opposite the lip. In the flush inlet, this location experiences the most severe fluid-turning on the scoop. It is also in the minimum area of the flowfield, hence the lowest static pressure area. In evaluating the problem, we compare the local static pressure near the lip with a static pressure in an undisturbed section of the freestream flow. Results are shown in Figs. 16a and 16b. The flush inlet tested is much more susceptible to cavitation than the scoop inlet, and in both inlets the pressure at the sensitive location is strongly affected by V_1/V_o, the velocity ratio. Drag data indicate the need for high V_1/V_o values, while cavitation data indicate that low values are required. Neither data indicate any particularly strong influence of the boundary-layer thickness.

External cavitation (resulting from the presence of the inlet) will most likely occur in the vicinity of the lip at the minimum pressure point of an equivalent airfoil. When fairing is adequate, external cavitation probably will also occur at the corners or intersections of the scoop and the hull. This cavitation can have two extremely harmful effects, increased drag and severe structural damage.

Fig. 18 Waterjet rotor. On the scale beneath the rotor, each unit represents 1 in.

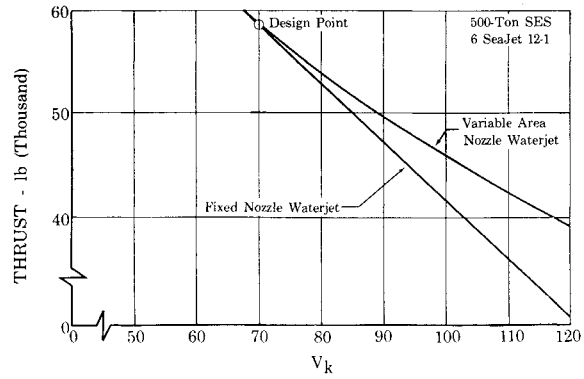

Fig. 19 Fixed-nozzle vs variable-nozzle waterjet performance.

Hydrofoil inlet designs face the same problems as displacement hull inlet designs, except that the inflow is generally planar. Hydrofoil inlets are further complicated by the fact that the inlet nacelle incorporates foil structural and actuating mechanisms. In addition, usually there is a 90° turn immediately after ingestion of the water.

External diffusion on a hydrofoil inlet results in high internal efficiencies (>90%) and high drag. The takeoff problem in hydrofoils, where maximum power and, thus, flow are required, occurs at minimum inlet pressure and has a strong influence on nacelle sizing. A possible solution is incorporation of an auxiliary scoop to capture as much ram pressure as possible, and in the closed position, to reduce drag as much as possible. (See Fig. 17.)

Waterjet Designs

Design of the waterjet itself can be, and has been, accomplished in several different ways. Any efficient pump can be used in a waterjet system, including centrifugal, mixed-flow, axial-flow, or propeller pump. The problem is to attain high efficiency at low inlet pressures, while avoiding cavitation damage.

Our solution is an axial-flow rotor with varying hub radius and high-solidity blading. The number of blades is minimized to improve cavitation performance. Figure 18 shows such a waterjet rotor. A typical feature of such pumps compared to classical axial-flow units is the low inlet flow coefficient. The flow coefficient is a direct result of rocket-inducer experience which, as in propoellers, shows improved cavitation performance with inlet blade angle reduced.

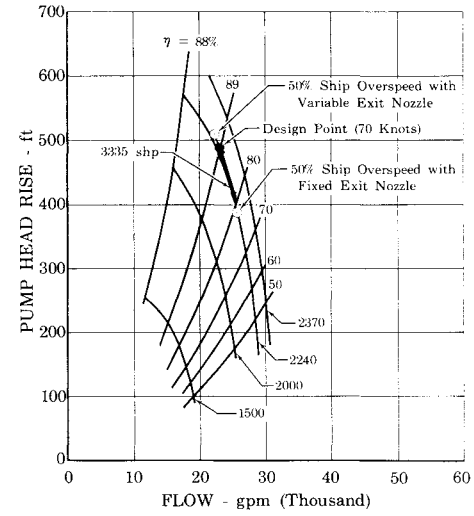

Fig. 20 Variable-nozzle effects on pump performance.

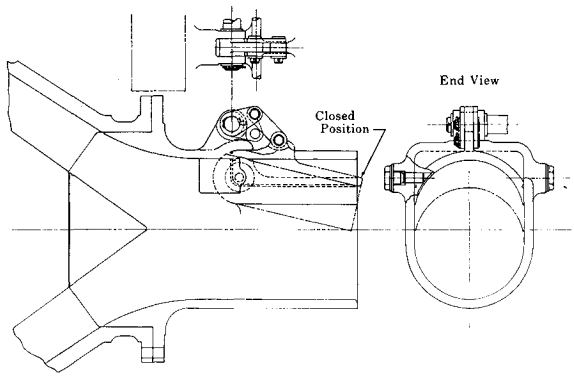

Fig. 21 Variable-geometry nozzle.

Waterjet nozzle designs are, for the most part, simple low-loss, fixed-area, converging nozzles. Their performance is depreciated seriously only when the flow from the pump stator contains appreciable rotational vectors or swirl, which is intensified by the nozzle contraction and can choke the pump flow.

Variable-area nozzles for waterjets are needed for vessels with a widely varying speed range, and when the inlet ram pressure is a significant portion of the system pressure. Under these conditions, changes in vessel speed cause significant changes in pump flow and tend to drive the unit into off-design conditions. By varying the nozzle area, the pump flow can be adjusted so that the pump operates at best efficiency. Figure 19 shows the effect of variable-area nozzles on thrust for a ship designed for 70 knots when it is operating at higher speeds. At 100 knots, the variable nozzle design gives 15% more thrust than the fixed nozzle. Figure 20 is a typical pump map that shows the extent of overflow and efficiency change at a 50% vessel overspeed. The variable-area nozzle can correct this overflow and adjust the jet velocity ratio to its optimum value. Mechanically, such nozzles are relatively straightforward designs. Figure 21 shows a variable geometry nozzle. Many other schemes are possible.

References

[1] Arcand, L., "Waterjet Propulsion for Small Craft," Small Craft Hydrodynamics Southeast Section Meeting, May 27, 1966, Society of Naval Architects and Marine Engineers.

[2] Traksel, J. and Beck, W. E., "Waterjet Propulsion for Marine Vehicles," Paper 65-245, 1965, AIAA; also *Journal of Aircraft*, Vol. 3, No. 2, March–April 1966, pp. 167–173.

[3] Wislicenus, G. F., "Hydrodynamics and Propulsion of Submerged Bodies," *ARS Journal*, Vol. 30, No. 12, Dec. 1960.

[4] Mossman, E. A. and Randall, L. M., "An Experimental Investigation of the Design Variables for NACA Submerged Duct Entrances," RMA7130, Jan. 1948, NACA.

[5] Hoerner, S. F., *Fluid Dynamic Drag*, Hoerner, Midland Park, N. J., 1958, pp. 9–16.

[6] Thurston, S. and Evanvar, M. S., "Efficiency of a Propulsor on a Body of Revolution Inducting Boundary-Layer Fluid," *Journal of Aircraft*, Vol. 3, No. 3, May 1966, pp. 270–277.

[7] Gearhart, W. S. and Henderson, R. E., "Selection of a Propulsor for a Submersible System," Paper 65-232, 1965, AIAA; also *Journal of Aircraft*, Vol. 3, No. 1, Jan.–Feb. 1966, pp. 84–90.

JANUARY 1968 J. HYDRONAUTICS VOL. 2, NO. 1

Prediction of the Seakeeping Characteristics of Hydrofoil Ships

IRVING A. HIRSCH*
The Boeing Company, Seattle, Wash.

Three methods for predicting the foilborne seakeeping characteristics of fully submerged-foil hydrofoil ships are presented. Each method uses an analog computer simulation of a hydrofoil ship and its sea-state environment. The first method, applicable only to regular waves, uses a sinusoidal representation of the sea. The second method is based on a statistical description of the wave height and orbital particle velocity. In the third method, the simulated ship's response to selected sinusoidal waves is combined with the spectral density function of wave height to yield a prediction of the ship's seakeeping characteristics in irregular waves. Each of the three methods has been used successfully in designing and evaluating automatic control systems for hydrofoil ships. Representative samples of seakeeping predictions obtained by each method are presented.

Introduction

HIGH-SPEED operation with good seakeeping characteristics forms the basic justification for the submerged-foil hydrofoil ship. The ability to predict the behavior of the hydrofoil ship in a given sea state is an important element in the design of the ship, and specifically, in the design and evaluation of the ship's automatic control system. The purpose of this paper is to describe three analytical techniques that can be used in predicting the foilborne seakeeping characteristics of submerged-foil hydrofoil ships.

Each of the methods presented uses a comprehensive electronic analog computer simulation of the hydrofoil ship and of the sea-state environment. In the simulation, the wave height and wave orbital particle velocity are represented. Both of these wave properties act as disturbances on the simulated ship. A simulated 70-ton preliminary-design hydrofoil ship is used in this paper as a basis for the presentation of computer predictions.

Presented as Paper 67-352 at the AIAA/SNAME Advanced Marine Vehicles Meeting, Norfolk, Va., May 22–24, 1967; submitted June 8, 1967; revision received October 23, 1967. The author wishes to thank J. D. Burroughs, R. M. Hubbard, and J. J. Jamieson for their helpful comments in preparing this paper.

* Associate Research Engineer, Controls Staff, Advanced Marine Systems, Aerospace Group.